

## Experimental Determination of Dynamic Characteristics of a Vibration-Driven Robot

Ivan A. Loukanov<sup>1</sup>, Svetlin P. Stoyanov<sup>2</sup>

<sup>1</sup>Department of Mechanical Engineering, University of Botswana, Botswana,

<sup>2</sup>Department of Technical Mechanics, University of Ruse, Bulgaria

---

**Abstract :** This paper presents the experimental determination of dynamic characteristics of a vibration-driven robot. The mechanical system consists of a shaker and a chassis. The latter is mounted on wheels furnished with one-way bearings build into the wheels hubs. The robot is propelled by the resonance vibrations created by the shaker's rotating masses, which generate propulsive impulses transmitted to the chassis. The latter were modified by the one-way bearings to unidirectional impulses thus creating a forward motion. By measuring and analyzing the accelerations of free damped oscillations of the propulsion system, when the chassis is fixed, the mechanical parameters such as spring constant, natural frequency and the damping factor were obtained. Moreover the resonance vibrations created by the shaker and the forced oscillations imposed to the chassis were recorded when the robot is moving unloaded. By employing the FFT tool box of the MATLAB software the frequencies and the magnitudes of accelerations of the shaker, the chassis and their relative accelerations were obtained. Lastly another series of tests were conducted when the robot is loaded by its towing force and accelerations and the towing force were measured and analyzed by using the FFT analysis.

**Keywords:** Resonance vibrations, inertia propulsion, one-way bearing, spring system, linear damping.

---

### I. Introduction

For many decades the Nuclear and Chemical industry, the Military and the Navy experienced shortages of robots which could be employed for observing, measuring, repair of pipes, air ducts and narrow channels, caves, as well as for discovery and destroying land and underwater mines, unexploded shells etc. The vibration-driven robots are cheap to manufacture, easy to control and propel through different environments, because of the simplicity of their design and operation capabilities. They require less power and develop strong traction as their propulsion is achieved by means of resonance vibrations of a specially designed one-degree-of-freedom excitation system [1, 2]. On the other hand the new propulsion systems prevents the robot from getting trapped in obstacles or on soft surfaces under the wheels [3] because the propulsion is created by means of internally provided impulses applied to the chassis, thus no-torques are acted upon the wheels as in conventional vehicles. Recently many academics are undertaking research in the field of mobile robots making an effort to invent new methods of propulsion based on friction forces, rotating masses or rectilinear moving masses inside of the robot [4], or designing and studying jumping robots by using the motion of two internally moving masses [5, 6], or employing the difference between static and kinetic friction [7, 8, 9], etc.

This study is dedicated to an experimental determination of dynamic (mechanical) parameters of a vibration-driven robot propelled by forced vibrations of a specially arranged propulsion system acting in the direction of referred motion. The anticipated direction of motion is achieved by using one-way bearings (clutches) mounted into the wheels hubs. They allow rotation of the wheels in one direction and prevent rotation in the opposite one. The accomplished motion has a pulsing nature and utilizes only less than 50% of the input energy to the oscillating system. By testing the robot and identifying the parameters of the system we expect improving the performance of the propulsion system and maximizing its efficiency.

Therefore the objective of this study is to measure and analyze the free damped and force oscillations of the shaker and the chassis of a prototype robot in order to determine the unknown mechanical and dynamic parameters of the propulsion system such as natural damped frequencies, equivalent spring stiffness, logarithmic decrement, coefficient of viscous resistance, damping coefficient, frequencies, accelerations etc.

### II. Materials and Method

The object of this study is the mobile wheeled robot illustrated in Fig. 1. It is intended for inspections and observations of air ducts or any other restricted environments where human do not have a direct access. Furthermore it may be used in a dangerous military, chemical or radiation sites, such as nuclear power stations, chemical reactors etc. This is the same mobile robot vehicle investigated and primarily tested in the studies [1, 2]. A similar configuration of a mobile motor vehicle is proposed by Goncharevich [3] with some design differences. However it has never been constructed or investigated so far. Apart of this the author is liable to

declare that the idea for the propulsion system of the robot was solely his own and it was developed independently before receiving a copy of the book [3] and reading the contents.

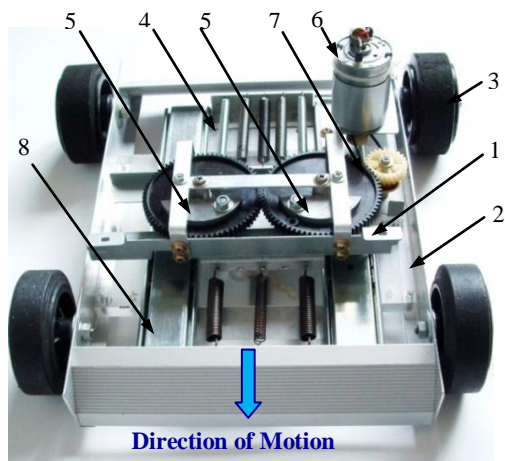


**Fig. 1** shows a front view of the wheeled robot, where: 1 - is the shaker; 2 - the chassis; 3 - one-way bearing installed in the hub of each wheel; 4 - spring system; 5 - rotating masses; 6 - DC motor; 7 - timing belt-gear drive transmission from the motor to the shaker; 8 - linear bearings.

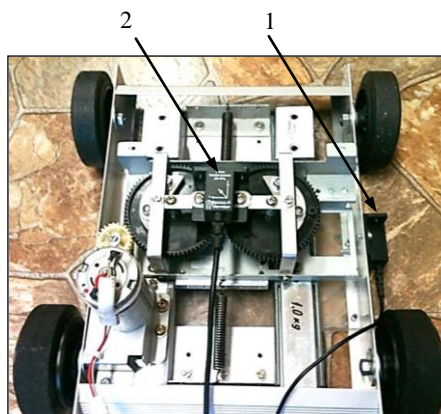


**Fig. 2** reveals the mounting locations of the accelerometers: # 1 which is **1D** - accelerometer ( $a_{max} = 25g$ ) fixed to the outer frame (the chassis) and # 2 is **3D** - accelerometer ( $a_{max} = 5g$ ) mounted on top of the shaker, where  $g=9.81 \text{ m/s}^2$ .

In reference to Fig. 1 the robot vehicle is propelled by a vibration excitation system, consisting of a small laterally balanced mechanical shaker of total mass -  $m_2$ , generating longitudinal inertial forces by means of two offset synchronously rotating opposite to each other masses -  $m_3$ . The excitation system (shaker) is placed on two linear bearings and connected to the chassis of the robot having a mass -  $m_1$  by means of ten equal and symmetrically placed tension springs of overall stiffness -  $k$  (See Fig. 4). The spring system is set to have an initial pre-tension such that its deflection is larger than the resonance amplitudes of the oscillating system. The generated propulsion forces by the shaker are transmitted to the chassis through the springs and the damping properties of the spring material.

For the purposes of determining the parameters of the system, the robot was equipped with two accelerometers one fixed to the chassis and the other one to the shaker as illustrated in Fig. 2. The accelerometers are intended for continuous measuring of the accelerations of the free damped and forced vibrations in the direction of motion of the shaker and the chassis. They are of piezoelectric type and are connected to a measuring and data-log electronic system of the Vernier Software & Technology © - LabQuest 2. Fig. 2 shows the locations of accelerometers and the methods of attachment (firmly fastened) to the respective oscillating bodies as well as their capacities in terms of maximum accelerations, measured in numbers of the gravitational acceleration,  $g=9.81 \text{ m/s}^2$ . Separately the measuring and data-log system used in this experimental study is illustrated in Fig. 3, showing its major features, technical provisions and properties of the USB ports. Some of technical data of the LabQuest 2 system are listed in Table 1 showing its specifications and limitations.

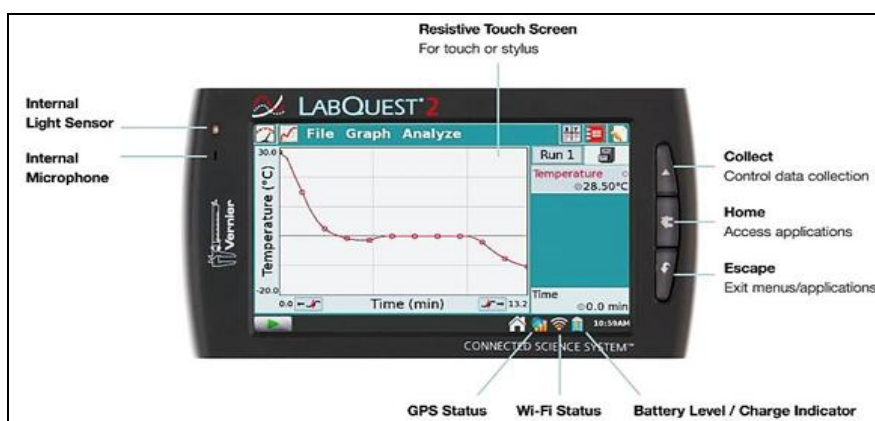


**Fig. 3** displays the LabQuest 2 measuring and data log system and presents its features

**Table 1 Major technical specification of the portable LabQuest 2 data-log and measuring system**

Processor	800 MHz
Communications	Wi-Fi 802.11 b/g/n; Bluetooth Smart for WDSS and Go Wireless Temp.
Interface	Resistive touch screen; Touch and stylus navigation for efficiency and precision.
Data Recording	Speed: 100,000 sps (samples per second); Resolution: 12-bit; Built-in GPS, 3-axis acc.
Memory	Imbedded: 200 MB; External: MicroSD, USB flash drive.
Ports	5 USB ports; flash & component ports; DC power jack; MicroSD/MMC; Audio In & Out
Accelerometers that can be used	Power supply: 30 mA, 5 VDC; Scope: $\pm 49 \text{ m/s}^2$ ( $\pm 25 \text{ g}$ ); Accuracy: $\pm 0.5 \text{ m/s}^2$ ( $\pm 0.05 \text{ g}$ ); Frequency range: 0–100 Hz; Resolution: $0.037 \text{ m/s}^2$

### III. Experimental study of the free damped oscillations of the robot propulsion system

To determine the dynamic parameters of the robot propulsion system (shaker), the chassis of the robot was fixed to the ground. The corresponding mechanical model is shown in Fig. 4 with the three masses involved, the equivalent spring stiffness  $k$  and the coefficient of viscous resistance  $b$ . At that point the spring system of the shaker is subjected to initial deflection bigger than the maximum amplitude of the oscillating system and released with zero initial velocity. At this time the excitation system begins free damped oscillations with its natural frequency until they fully vanished. During the excitation of the shaker the signal measured by the #2 accelerometer was continuously recorded until it disappeared. The experiments were repeated three times and then the recorded signals were separately analyzed. The individual parameters of the propulsion system were estimated by using the recorded signals such as amplitudes, periods, frequencies etc. and others were calculated according to the well-known equations.

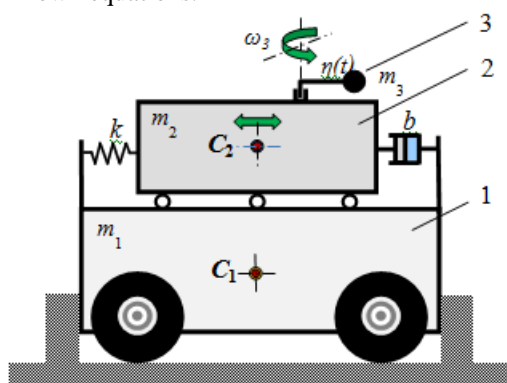


**Fig. 4** presents the mechanical model used for measuring the free damped & forced oscillations of shaker; where 1 is the chassis (body1 of mass  $m_1$ ); 2 – shaker (body 2 of mass  $m_2$ ), 3 - two synchronously rotating masses -  $m_3$ .

#### 3.1 Mechano-mathematical model used in the free damped oscillations of the robot propulsion system

In this case we are considering the robot propulsion system as one-degree-of-freedom. The choice of the mathematical model is disputable, but we choose as a first approximation the linear model, where the spring force is proportional to its deflection and the resisting force is proportional to the velocity of oscillations, as presented in Fig. 5 below. When free oscillations are investigated the chassis is fixed and the rotating masses are non-rotating but participating in the free oscillations of the shaker.

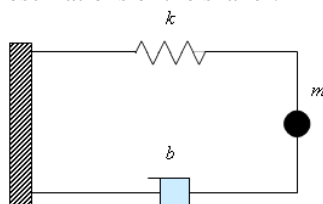


**Fig. 5** presents the mathematical model of the excitation system, of bodies 2 and 3, where  $m=m_2+m_3$

The linear model is governed by the homogeneous ordinary differential equation of second order, written as:

$$m\ddot{x}_2 + c\dot{x}_2 + kx_2 = 0 \tag{1}$$

where:  $m=m_2+m_3$  is the oscillating mass of the excitation system (shaker), including the mass of the rotating eccentric masses  $m_3$  and the spring system.

We also introduce the ratios:

$$\ddot{x}_2 = d^2x_2/dt^2 \text{ and } \dot{x}_2 = dx_2/dt, \tag{2}$$

$$b/m = 2n \text{ and } k/m = \omega^2$$

which are the second and the first time derivatives of the displacement  $x_2$  with respect to time,  $b$  is the coefficient of viscous resistance [N.s/m],  $k$  is the stiffness of the equivalent spring [N/m] and:

$$b/m = 2n \text{ and } k/m = \omega^2 \tag{3}$$

In (3),  $n=b/2m=\delta.f$ , [rad/s] is the damping coefficient of the oscillating system and  $\omega$  [rad/s] is the angular frequency of the damped oscillations. The magnitude of the oscillating mass of the shaker is  $m = (m_2+m_3) = 1.31$  kg, where  $m_2=1.19$  kg and  $m_3=0.12$  kg. Also the equation of logarithmic decrement is employed in calculating the damping coefficient  $n$  as per the known equation:

$$\delta = (1/3) \ln [(a_i/a_{i+3})] \tag{4}$$

### 3.2 Experimental investigation of the free damped oscillations of the robot propulsion system

**Figs. 6 & 7** and **Figs. 8 & 9** exemplify the recorded free damped oscillations of the excitation system being the propulsion system of the robot. The system has total oscillating mass  $m=1.31$  kg and is connected to the chassis by means of 10 same size and same stiffness helical tension springs. All the experiments of free damped oscillations were conducted at the same mechanical setup and the oscillations were generated by shifting the system from equilibrium position to its maximum position and releasing it from rest. In this case the eccentric masses  $m_3$  were stationary (not rotated) and oscillating together with the shaker (body2).

In this series of experiments, experiment #1 was unsuccessful because it was accompanied by a high frequency ripple of unknown origin. So we will discuss and analyze the experiments #2, #3 and #4 only. Each of the experiments was analyzed by using two reference points from the recorded signal. This approach allows getting better accuracy when evaluating each record.

In the following figures the first reference points are shown in blue color and the second points in red color. The corresponding values of the time and the accelerations are listed in Table 2. The time interval is used to calculate the frequencies and the magnitudes of accelerations in order to calculate the logarithmic decrement -  $\delta$ . The value of the decrement is employed to calculate the damping coefficient of the oscillating system by means of the frequencies of oscillations, also obtained from this experiment.

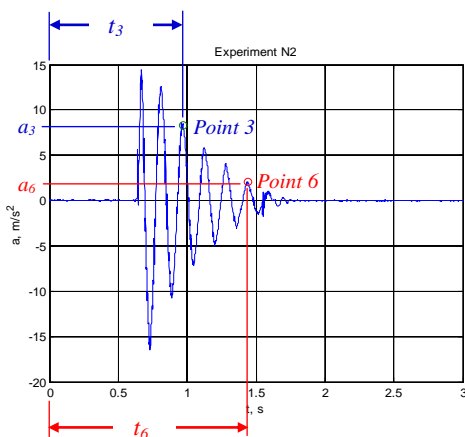


**Fig. 6** gives details for the free damped oscillations of experiment #2 where data are taken from reference points 3 and 6

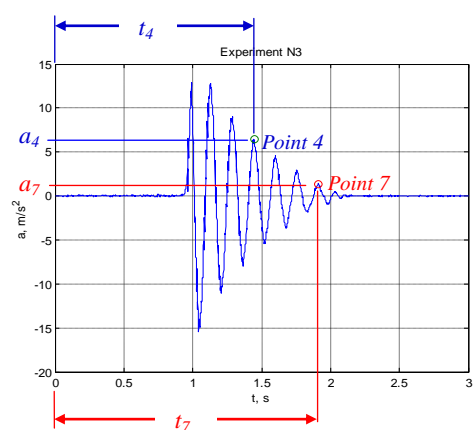


**Fig. 7** exhibits free damped oscillations recorded from experiment #3 where data are taken from reference points 4 and 7

In Fig. 6 (exp. #2) and Fig. 8 (exp. #4) the reference points 3 and 6 were used for determining the system parameters as shown. The respective time instances  $t_3$  and  $t_6$  and the associated accelerations  $a_3$  and  $a_6$  are illustrated in the graphs. Fig. 7 (exp. #3) indicates the related reference points 4 and 7, the time instances  $t_4$  and  $t_7$ , as well as the corresponding accelerations of the free damped oscillations  $a_4$  and  $a_6$ .

By using the magnitudes of the accelerations at a particular time instant corresponding to the respective reference points shown in the above figures the system parameters were determined and listed in Table 2. The measured and processed data are finally averaged for the three experiments of the oscillating system.

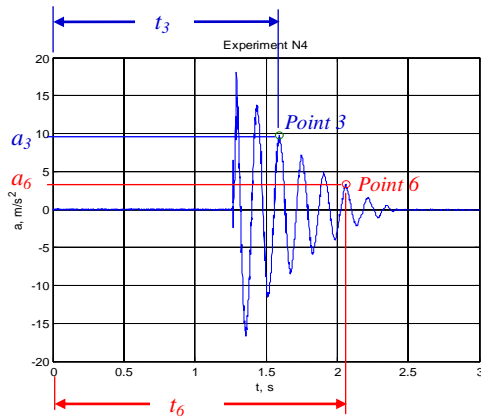


Fig. 8 shows details of the free damped oscillations of experiment #4 where data are taken from reference points 3 and 6

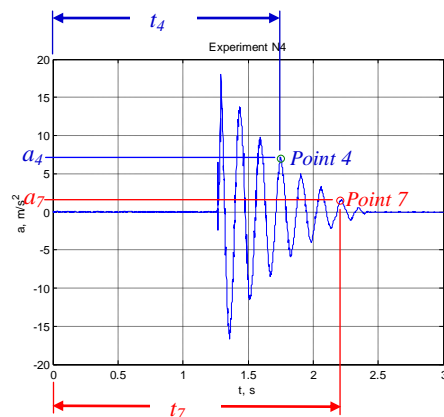


Fig. 9 shows details of the free damped oscillations of experiment #4 where data are taken from reference points 4 and 7

It should be mentioned ones again that the parameters obtained from experiment #2 are based upon reference points 3 & 6 and that of experiment #3 upon reference points 4 & 7. Also the parameters found from experiment #4 were evaluated twice by using the data drawn from reference points 3 & 6 and after that from points 4 & 7 as shown in Fig. 8 and Fig. 9 respectively. The reason for this approach is to account for the fact that the results may vary when different reference points are employed within the same record. This method allows getting better accuracy and eliminates the variation of the period due to some non-linear effects not accounted for by the linear model shown in Fig. 5. The same approach could be used for experiments #2 and #3, but due to constrained space in the paper it is done for experiment # 4 only.

Table 2 Test results from experiments # 2, #3 and #4 for m = 1.31 kg (free damped oscillations)

Parameters of the oscillating system	Equations and units	Values of parameters				Avg.
		Exp. #2 (p. 3-6)	Exp. #3 (p. 4-7)	Exp. #4 (p. 3-6)	Exp. #4 (p. 4-7)	
Initial reference point, #3	$t_3$ [s]	0.969	/	1.593	/	/
Final reference point, #6	$t_6$ [s]	1.441	/	2.061	/	/
Initial reference point #4	$t_4$ [s]	/	1.445	/	1.750	/
Final reference point, #7	$t_7$ [s]	/	1.911	/	2.210	/
Period of free undamped oscillations,	$T = (t_6 - t_3)/3$ [s]	0.157	/	0.156	/	<b>0.155</b>
Period of free undamped oscillations,	$T = (t_7 - t_4)/3$ [s]	/	0.155	/	0.153	
Frequency of the free damped oscillations	$f = [1/(t_6 - t_3)]/3$ [Hz]	6.356	/	6.410	/	<b>6.432</b>
Frequency of the free damped oscillations	$f = [1/(t_7 - t_4)]/3$ [Hz]	/	6.438	/	6.522	
Acceleration corresponding to point #3	$a_3$ [m/s <sup>2</sup> ]	8.307	/	9.815	/	/
Acceleration corresponding to point #6	$a_6$ [m/s <sup>2</sup> ]	2.028	/	3.325	/	/
Acceleration corresponding to point #4	$a_4$ [m/s <sup>2</sup> ]	/	6.447	/	6.939	/
Acceleration corresponding to point #7	$a_7$ [m/s <sup>2</sup> ]	/	1.326	/	1.432	/
Circular frequency of the damped system	$p = 2\pi f$ [s <sup>-1</sup> ]	39.936	40.450	40.277	40.977	<b>40.41</b>
Logarithmic decrement, Exp. #2 and #4 and Exp. #3 & #4	$\delta = (1/3) \cdot \ln(a_3/a_6)$	0.470	/	0.361	/	<b>0.471</b>
	$\delta = (1/3) \cdot \ln(a_4/a_7)$	/	0.527	/	0.526	
Coefficient of damping	$n = \delta \cdot f$ [s <sup>-1</sup> ]	2.988	3.391	2.313	3.430	<b>3.031</b>
Coefficient of viscous resistance	$b = 2mn$ [Ns/m]	7.679	8.715	5.944	8.815	<b>7.788</b>
Circular frequency of the damped system	$\omega = \sqrt{(n^2 - p^2)}$ [s <sup>-1</sup> ]	39.824	40.307	40.210	40.833	<b>40.29</b>
Natural frequency of the damped system	$f_\omega = \omega/(2\pi)$ [Hz]	6.338	6.415	6.400	6.499	<b>6.413</b>
Coefficient of equivalent stiffness	$k = m_2 \cdot \omega^2$ [N/m]	2037.9	2087.7	2077.7	2142.6	<b>2086</b>



**Fig. 10** illustrates the equipment used in the forced vibration test, where: 1 is the shaker (body 2); 2 - LabQuest 2 unit, 3 – the power supply unit, 4 - motor speed controller: 5 - accelerometer # 2

### 3.3 Experimental investigation of forced vibrations of shaker when the chassis is fixed.

New series of experiments were conducted with the robot propulsion system shown in Fig. 4 where the chassis, body1, is fixed to the ground and body2 (shaker) subjected to forced oscillations generated by the rotating eccentric masses  $m_3$ . This is achieved by controlling the speed of the DC motor by means of a speed controller such that the single-degree-of-freedom oscillating system approaches the resonance along the ascending branch of the resonance graph. As a result the amplitudes of displacement, velocities and accelerations of body2 (shaker) attained maximum values. During this time the signal generated by the accelerometer #2 was continuously recorded for four seconds and saved by the LabQuest 2 data log system. After that it was analyzed with the Fast Furries Transform (FFT) tool box of the MATLAB software.

**Fig. 10** shows the experimental setup used for the forced oscillations done with the robot propulsion system. The differential equation governing the forced vibrations of the oscillating system is:

$$m\ddot{x}_2 + c\dot{x}_2 + kx_2 = m_3\rho\omega^2 \sin(\omega t) \quad (5)$$

where:  $m=m_2+m_3$ , is the shaker oscillating (propulsion) mass and  $\rho$  is the offset from the axis of rotation of the unbalanced rotating masses, having total mass  $m_3=0.12$  kg.

Two experiments were conducted with the chassis (body1) being fixed to the ground while the propulsion system (shaker) is running in close to resonance condition. It is always difficult to set the supplied voltage to the motor of the same magnitude. For this reason most of the repeated experiments experience slightly different magnitudes of accelerations and amplitudes of resonance oscillations.

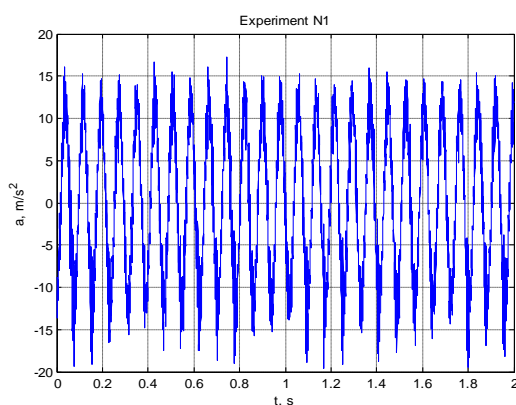


**Fig. 11** illustrates the relative resonance oscillations of body2 with respect to the fixed body1 during Exp. # 1

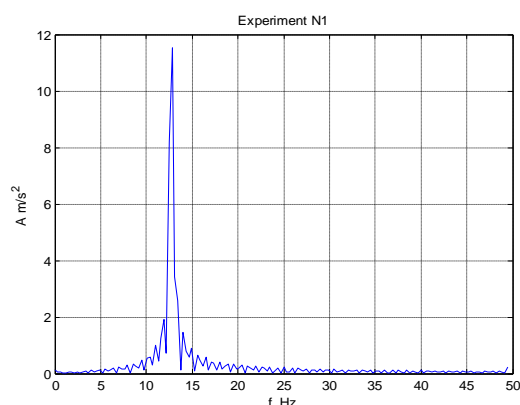


**Fig. 12** exemplifies the spectrogram of the relative resonance oscillations of body2 with respect to the fixed body1

**Figs. 11** and **13** present the recorded force oscillations while **Figs. 12** and **14** demonstrate the corresponding spectrograms obtained from the FFT analysis for experiments #1 and #2 respectively. From the spectrogram in **Fig. 12** shows the frequency of relative oscillations and the amplitude of the acceleration of body2 with respect to the fixed body1 are found to be  $f_{rel} = 12.82$  Hz and  $a_{rel} = 11.53$  m/s<sup>2</sup>.

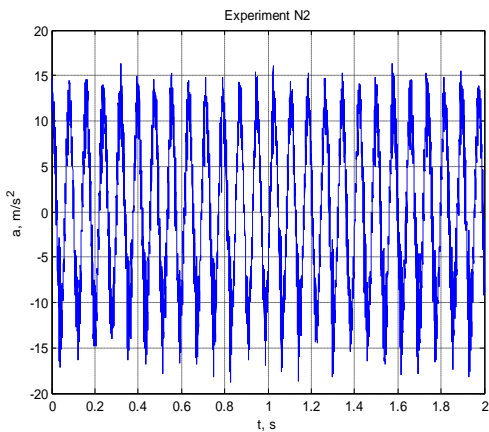


**Fig. 13** illustrates the relative resonance oscillations of body 2 with respect to the fixed body 1 during Exp. # 2

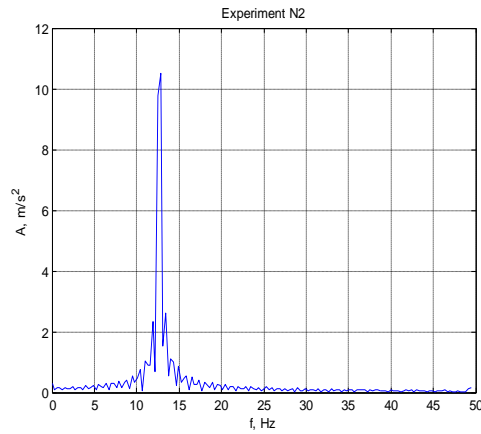


**Fig. 14** shows the spectrogram of the relative oscillations of body2 with respect to fixed body1 during Exp. # 2

Likewise from the spectrogram in Fig. 14 similar to that in Fig. 12 the frequency of forced oscillations and the amplitude of the accelerations of body2 relative to the fixed body1 are found to be  $f_{rel} = 12.82$  Hz and  $a_{rel} = 10.51$   $m/s^2$  respectively. The difference in the accelerations is owing to the different voltage set up supplied to the motor, hence small differences result in the generated accelerations for the same resonance frequency of the shaker. Obviously the frequencies are not affected by the voltage deviation supplied to the DC motor, only the amplitudes of accelerations are sensitive to that. The reason is that at different locations on the ascending portion of the resonance graph, the magnification changes significantly, hence the accelerations vary.

**Table 3** Experimental data of forced oscillations of body 2 regarding the fixed body 1

Number of experiment	Frequency, $f_1=f_2$ , [Hz]	Circular freq. $\omega_2$ , [rad/s]	Acceleration, $a_2=A$ , [ $m/s^2$ ]	Average acceleration, $A_{2avg} = A=(a_{2\#1}+a_{2\#2})/2$ , [ $m/s^2$ ]
Exp. # 1	12.82	80.53	11.53	11.02
Exp. # 2			10.51	

#### IV. Experimental investigation of forced vibrations of unloaded robot in motion.

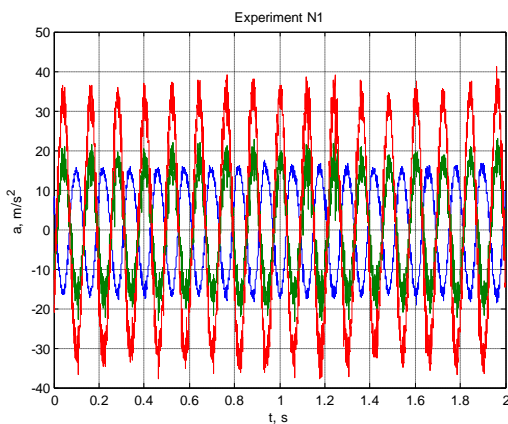


**Fig. 15** illustrates the recorded signals of forced oscillations of body1 (blue), body2 (green) and the relative acc. (red) between body1 and body2, from exp. #1

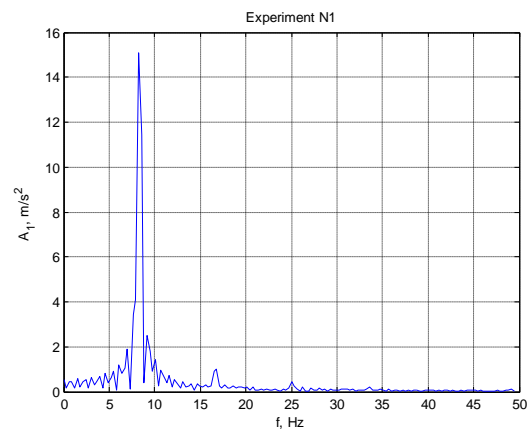


**Fig. 16** presents the frequency spectrogram of body1 (chassis) obtained from exp. #1 when the unloaded robot is in motion,  $f_1 = 8.24$  Hz &  $a_1=A_1 = 15.07$

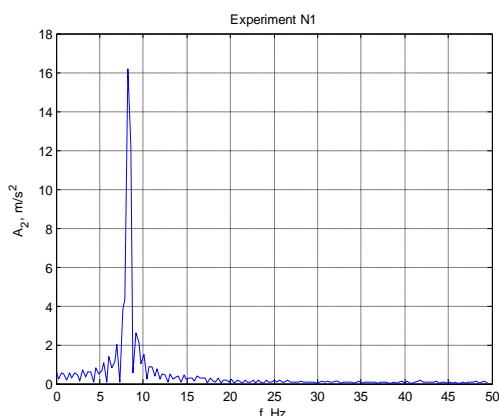


**Fig. 17** displays the frequency spectrogram of body2 (shaker) obtained from Exp. #1 when the unloaded robot is in motion,  $f_2 = 8.24$  Hz and  $a_2=A_2 = 16.16$

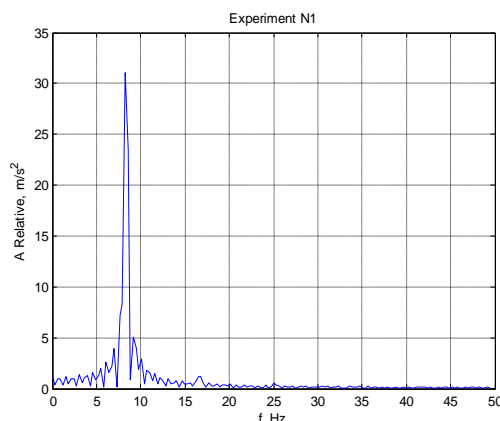


**Fig. 18** shows the spectrogram of the relative motion of body2 relative to body1 from Exp. #1 of the unloaded moving robot,  $f=8.24$  Hz,  $a=A= 31.02$  m/s<sup>2</sup>

Two experiments were conducted with the unloaded robot in motion. The objective is to analyze the interactions between the forced oscillations of body2 and that of body1 as well as their relative interactions. Fig. 15 shows the recorded oscillations from experiment #1 of body1 (blue), body2 (green) and the relative oscillations between bodies 1 and 2 shown in red color. Obviously the accelerations are poly-harmonic because of interactions between the bodies involved in the oscillating system. In this case the signals produced by the accelerometers attached to body1 (blue) and body2 (green) was recorded along with the generated relative oscillations (red). Next, these signals were analyzed with the FFT tool box of MATLAB software to produce the above spectrograms. These are shown separately in Figs. 16, 17 and Fig. 18.

It is remarkable that all bodies in the system oscillate with the same resonance frequency  $f_1 = f_2 = f = 8.24$  Hz but instead the amplitudes of their accelerations are dissimilar due to the difference in the power supply to the motor in each test. The relative amplitude of the acceleration appears to be approximately the sum of the accelerations of body1,  $a_1$  and body2,  $a_2$ , i.e.  $A \approx A_1 + A_2$  or  $a \approx a_1 + a_2 = 15.07 + 16.16 = 31.23$  m/s<sup>2</sup>  $\approx 31.02$  m/s<sup>2</sup>, or having only 0.61% difference. The difference in amplitudes is negligibly small and therefore it is neglected. So the determined amplitudes and frequencies are of good accuracy and may be used in the forthcoming theoretical studies of the same system and will give us an insight about the theoretically predicted dynamic parameters.

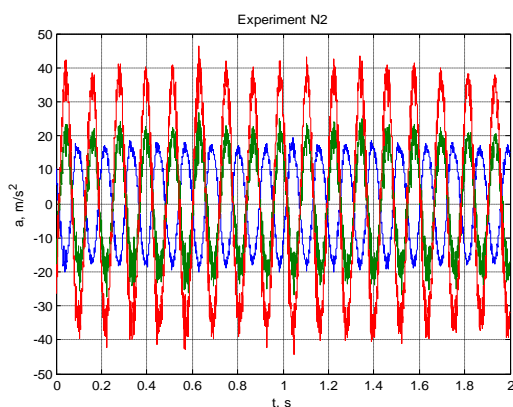


**Fig. 19** illustrates the recorded signals of forced oscillations of body 1 (blue), body 2 (green) and the signal of relative (red) acceleration between them from Exp. #2

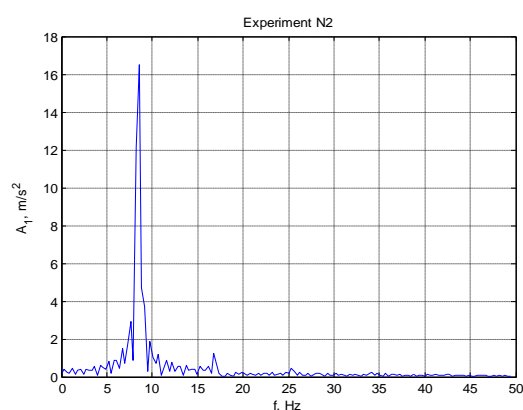


**Fig. 20** shows the frequency spectrogram of body1 (chassis) taken from Exp. #2 when the unloaded robot was in motion,  $f_1 = 8.54$  Hz and  $a_1=A_1 = 16.51$  m/s<sup>2</sup>

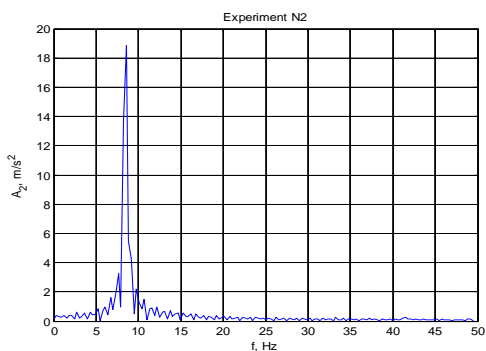


**Fig. 21** denotes the frequency spectrogram of body2 (green) from Exp. #2 when the robot is in motion, so the frequency  $f_2 = 8.54$  Hz & acceleration  $a_2=A_2 = 18.86$  m/s<sup>2</sup>

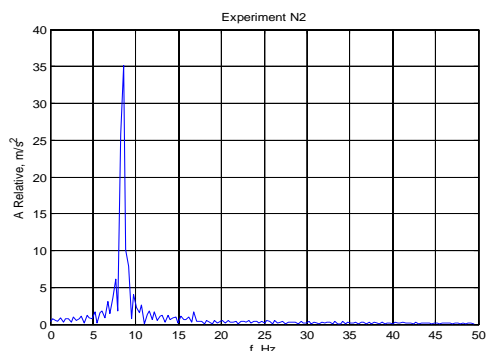


**Fig. 22** presents the spectrogram of the relative acceleration of body2 about body1 taken from Exp. #2 while the robot is moving, then  $f = 8.54$  Hz. and  $A = 35.14$  m/s<sup>2</sup>

From experiment #2, the recorded accelerations of body 1 and body 2 and the relative accelerations are presented in Fig. 19. The same colors codes were used in identifying the accelerations of the bodies as in Fig. 15 above. By analyzing the results of exp. #2 it was detected that the three accelerations have the same frequency  $f = 8.54$  Hz and the value of the relative acceleration is approximately the sum of the accelerations of the respective bodies: namely  $A \approx A_1 + A_2$ , or  $a \approx a_1 + a_2 = 16.51 + 18.86 = 35.38$  m/s<sup>2</sup>  $\approx 35.14$  m/s<sup>2</sup> as seen in the spectrogram of Fig. 22. The differences in test 1 and test 2 are 0.61% and 0.68% respectively, so these are too small and may be neglected. The experimental data obtained from experiments #1 and #2 are listed in Table 4.

**Table 4 Experimental results from forced oscillations of the moving unloaded robot – body1 and body2**

Number of Experiment #	Common frequency $f_1 = f_2 = f$ [Hz]	Acceleration of body 1 $a_1$ , [m/s <sup>2</sup> ]	Acceleration of body 2 $a_2$ , [m/s <sup>2</sup> ]	Relative acceleration between body 1 and body 2 $a_{rel}=A$ , [m/s <sup>2</sup> ]
Exp. # 1	8.24	15.07	16.16	31.02
Exp. # 2	8.54	16.51	18.86	35.14
Avg. of #1 and #2	8.39	15.79	17.51	33.08

The difference in the accelerations in these experiments is because of the different voltage supply to the motor for each setup leading to different values of the accelerations. As mentioned in section 3.3, it is difficult to set the system to the same resonance, so small variations in the values of accelerations and frequencies are likely.

### V. Experimental investigation of forced vibrations of the loaded robot in motion.

Five experiments were conducted as per the set up shown in Fig. 23. In all of them a load sell of  $\pm 10$  N is used to measure the towing force of the robot along with the accelerometers #1 and #2 measuring the accelerations of body1 and body2 respectively. The load sell is connected to body1 by means of a rubber string intended to damp (minimize) the fluctuations in the recorded force, although not fully succeeded.



**Fig. 23** illustrates the experimental set up where: 1 – is body1; 2 – body2; 3 – accelerometers #1; 4 – accelerometer #2; 5 – load sell; 6 – new power supply & speed controller; 7 – LabQuest 2 unit.

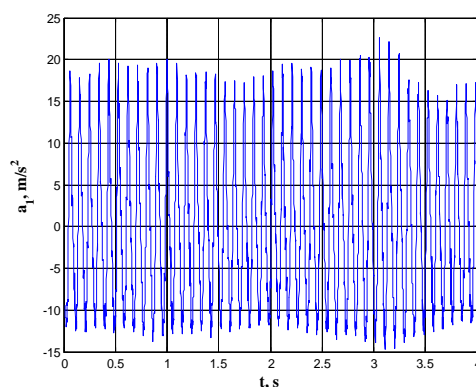


**Fig. 24** shows the pattern of acceleration of body1

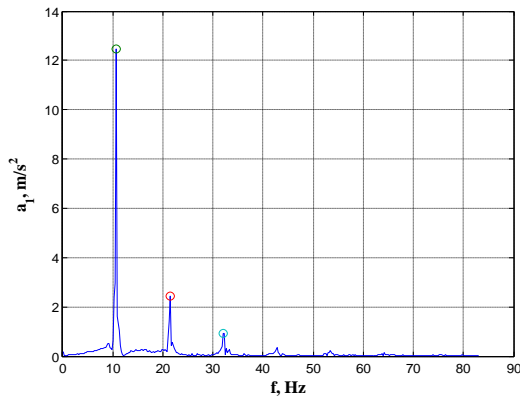


Fig. 25 displays the spectrogram of accelerations

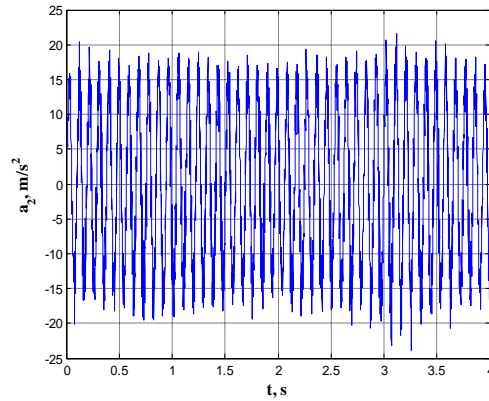


Fig. 26 shows the pattern of acceleration of body2

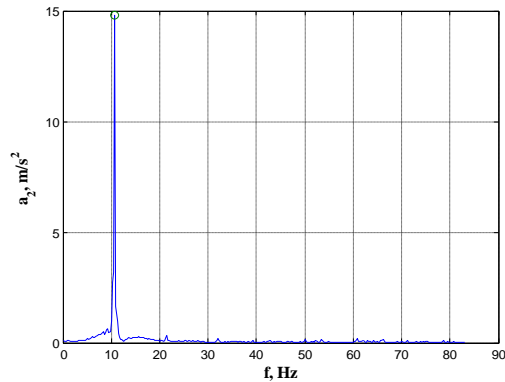


Fig. 27 identifies the main frequency of the acceleration of body2 with the rest being negligible

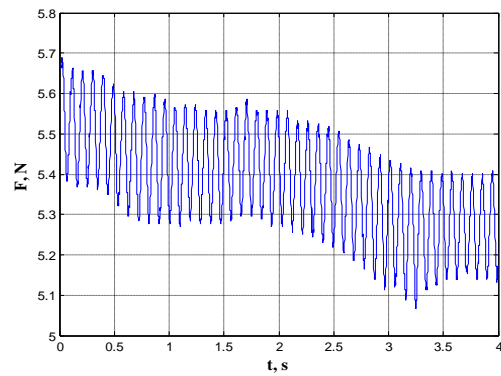


Fig. 28 illustrates the variation of the towing force  $F$  during test #1 for duration of 4 seconds

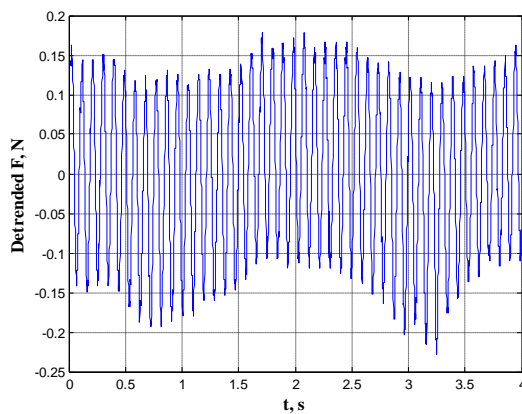


Fig. 29 shows the towing force  $F$  after being modified (detrended) by the FFT analysis.

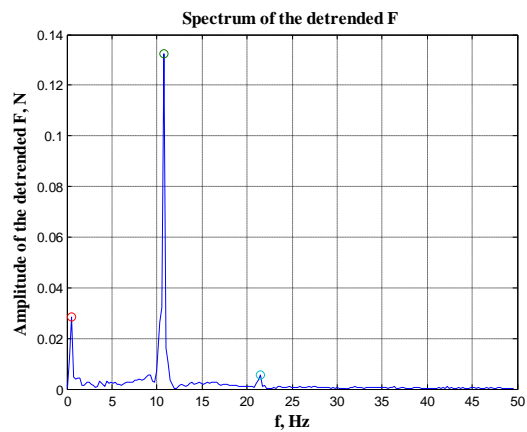


Fig. 30 specifies the main amplitude of towing force  $F$  with the rest of amplitudes being minor.

The experiments are done on a PV dry and horizontal surface under ambient temperature of 25 °C. Owing to the limited space in the paper only the graphs of experiment # 1 are shown. The rest of the tests results are listed in Table 5, where the values of the accelerations, frequencies and mean towing force are shown. For comparison purposes in addition to these data the last row in Table 5 repeats the average data taken from Table 4 for the unloaded robot's accelerations and frequencies of body1 and body2 respectively.

Table 5 Experimental data obtained from the loaded robot with its towing force and of unloaded robot

No. of exp.	Accelerations of Body1, m/s <sup>2</sup>	Accelerations of Body2, m/s <sup>2</sup>	Frequencies of Body1 Hz	Frequencies of Body2 Hz	Mean value of towing force, F N	Frequency of detrended force, Hz
No. 1	a <sub>1,1</sub> =12.5 a <sub>1,2</sub> =2.45 a <sub>1,3</sub> =0.93	a <sub>2</sub> =14.8 0 0	f <sub>1,1</sub> =10.7 f <sub>1,2</sub> =21.5 f <sub>1,3</sub> =32.0	f <sub>2</sub> =10.7 0 0	5.38	f <sub>1,1</sub> = 10.7 f <sub>1,2</sub> = 5.53 f <sub>1,3</sub> = 0.49
No. 2	a <sub>1,1</sub> =11.7 a <sub>1,2</sub> = 2.12 a <sub>1,3</sub> = 1.12	a <sub>2</sub> =15.3 0 0	f <sub>1,1</sub> =11.0 f <sub>1,2</sub> =21.7 f <sub>1,3</sub> =32.7	f <sub>2</sub> =11.0 0 0	4.99	f <sub>1,1</sub> = 11.0 f <sub>1,2</sub> = 0.49 f <sub>1,3</sub> = 21.7
No. 3	a <sub>1,1</sub> = 8.49 a <sub>1,2</sub> = 2.72 a <sub>1,3</sub> = 0.64	8.19 0 0	f <sub>1,1</sub> =10.3 f <sub>1,2</sub> =20.8 f <sub>1,3</sub> =31.0	10.3 0 0	5.42	f <sub>1,1</sub> =10.3 f <sub>1,2</sub> = 0.49 f <sub>1,3</sub> =20.8
No. 4	a <sub>1,1</sub> =11.6 a <sub>1,2</sub> = 2.39 a <sub>1,3</sub> = 1.07	10.4 0 0	f <sub>1,1</sub> =10.3 f <sub>1,2</sub> =20.5 f <sub>1,3</sub> =31.0	10.3 0 0	5.32	f <sub>1,1</sub> =10.3 f <sub>1,2</sub> = 0.49 f <sub>1,3</sub> = 20.8
No. 5	a <sub>1,1</sub> =13.0 a <sub>1,2</sub> = 2.05 a <sub>1,3</sub> = 0.96	12.3 0 0	f <sub>1,1</sub> = 9.76 f <sub>1,2</sub> =19.3 f <sub>1,3</sub> =29.1	9.76 0 0	5.14	f <sub>1,1</sub> = 9.76 f <sub>1,2</sub> = 0.24 f <sub>1,3</sub> =19.5
Avg. #(1 to 5)	a <sub>1,1,avg</sub> =11.5	12.2	f <sub>1,1,avg</sub> =10.4	f <sub>2,avg</sub> =10.4	F <sub>avg</sub> =5.25	f <sub>1,1,avg</sub> =10.4
Avg. #(1 to 2)	15.8	17.5	8.4	8.4	Unloaded Robot	

### VI. Discussion

In this paper an experimental investigation of a vibration-driven wheeled robot is conducted, studied and analyzed. The objective was to determine the dynamic (mechanical) characteristics of the robot propulsion system with the aim of employing these data in an upcoming study dedicated to the optimization of the robot system. The optimization technique will be based upon a Multicriteria parametric optimization method by using the determined parameters of the robot propulsion system in this study as a pilot data. The experimental results obtained from the free damped oscillation of the robot propulsion system (body2) were listed in Table 2. On the other hand the data of forced oscillations of body2 relative to the fixed body1 are recorded in Table 3. It was found that both bodies oscillate with the same forced frequency during the experiments but the magnitudes of their accelerations differ because of the slight difference in the voltage set up to the motor during each experiment. The latter forces the motor to operate with different speeds of rotation and hence dissimilar values of the individual accelerations are registered.

Furthermore the robot mechanical system was investigated during forced resonance oscillations of the propulsion system while the robot was moving with no towing force applied to it. The values of frequencies and amplitudes of the respective accelerations of body1 (chassis) and body2 (shaker) were identified by employing the FFT tool box of the MATLAB software. As a result the spectrograms showing the accelerations versus frequency were constructed and the data obtained from them are listed in Table 4. It is found again that the two bodies oscillate with the same frequency but have different accelerations, which relate to the difference in their masses and ones again due to different voltage supplied to the motor. Incredibly, it was also found that the relative acceleration between the shaker and the chassis appears to be the sum of the magnitudes of the respective bodies' accelerations, having about 0.61% to 0.68% difference. It was agreed to neglect that difference which is considered small and compatible with the accuracy of the experimental equipment. Another series of five experiments were conducted to investigate the accelerations and frequencies of the robot when it was in motion but subjected to its maximum towing force. This is done by using a load cell attached to body1 as shown in Fig. 23. The results of these experiments were listed in Table 5 and thoroughly analyzed to find out the effect of the towing force on the accelerations and resonance frequencies developed by the propulsion system of the robot when it is fully loaded. It is found that body1 and 2 oscillate with the same frequencies but have slightly different accelerations ones again due to somewhat different power supply in each experiment.

It is also discovered that body1 has three significant frequencies with the lowest one being 10.74 Hz. So the second significant frequencies of body1 is found to be twice the lowest one, mainly:  $f_{1,2}=2 \times (f_{1,1}=10.74) = 21.48$  Hz, and the third one is triple the lowest frequency, or  $f_{1,3} = 3 \times (f_{1,1}=10.74) = 31.98$  Hz. Therefore these frequencies appear to be multiple to the lowest frequency of body1. Finally the average frequency of body1 is found to be 10.4 Hz and the same applies to the frequencies of body2, which average frequency was constant equal to 10.4 Hz. Comparing the average accelerations and average frequencies of the moving robot without any towing force acting on it and the loaded robot listed in Table 5, it is found that the accelerations of body1 and body2 are 11.5 m/s<sup>2</sup> and 12. 2 m/s<sup>2</sup> respectively with their average frequencies being both equal to 10.4 Hz. On the other hand for the loaded moving robot the respective average accelerations are 15.8 m/s<sup>2</sup> and 17.5 m/s<sup>2</sup>, while their frequencies are the same but equal to 8.4 Hz. The analysis revealed that when the robot is loaded by the towing force the accelerations of body1 and body2 increased by 37.4 % and 43.4% respectively, while the average frequencies of their oscillations drop by 23.8%. These findings suggest that there is a significant interaction between the oscillations of the bodies in the system and the components become more stressed when the robot is loaded rather than when it is unloaded. Practically it means that there will be a possibility of

arranging the propulsion system in such a way so as to achieve and appropriate transmission of energy from body2 to body1 and minimize the inertial loads. This could be set by selecting appropriate spring stiffness, mass ratio and introduce an adequate damping in order to maximize the mean velocity of body1, increase the robot displacement per cycle of oscillations and the take full advantage of the towing force.

## VII. Conclusions

This paper presents the experimentally determined dynamic characteristics of a prototype wheeled robot, which physical model is shown in Figs. 1, 2 and Fig. 4 along with the measuring and data-log system illustrated in Fig. 3. The determined accelerations and frequencies of body1 and body2 are listed in Tables 2, 3, 4 and 5. They are of good accuracy due to the use of a sophisticated measuring and data-log system as well as using the analyzing FFT tool box in the MATLAB software. The results will be used in a forthcoming study of the same physical model of the robot as reference data and compared with the theoretically identified parameters of the system. However, if a modified vibration-driven robot is investigated, it would require conducting similar experimental study and analysis in order to obtain comparable parameters corresponding to the modified model. To improve the towing ability and the mean velocity of the mobile robot it may be recommended to conduct an optimization study and find out the influence of the individual dynamic parameters determined in this study upon the robot mean velocity and the towing force. Obviously a Multicriteria parametric optimization would be required as most of the determined parameters have significant influence upon the robot performance characteristics. On the other hand to improve the efficiency of the robot propulsion system it would require introducing another degree of freedom in the system. This eventually would have given the opportunity of utilizing part of the rest 50% of the input energy so far lost during the return stroke in the one-way bearings. In conclusions it may be stated that the experimental investigation described in this study provides important values for the dynamic parameters of the prototype robot. They would ultimately be employed in further optimization analysis to find out the optimum values of these parameters in order to maximize the mean velocity and the towing force of the robot, combined with reduced inertial loads upon the components of the system.

## Acknowledgments

This study was made possible thanks to the research Project FNI-RU, № 2015-MTF-01 funded by the University of Ruse, Bulgaria. The authors are sincerely grateful to V.G. Vitliemov, I.V. Ivanov, S.G. Stoyanov and V.S. Bozduganova from the department of Technical Mechanics for their continuous support and inspiration during the project development. The authors also express their gratitude to Mr. E.G. Stanev for his assistance.

## References

- [1]. Loukanov I. A., Vibration Propulsion of a Mobile Robot. IOSR Journal of Mechanical and Civil Engineering, Vol. 12, Issue 2 Version II, 2015, pp. 23-33, [www.iosrjournals.org](http://www.iosrjournals.org)
- [2]. Loukanov I. A., Application of Inertial Forces for generating Unidirectional Motion, Proceedings of the Scientific Conference of University of Ruse, Vol. 53, Series 2, 2014, (НАУЧНИ ТРУДОВЕ НА РУСЕНСКИЯ УНИВЕРСИТЕТ - 2014, Том 53, Серия 2).
- [3]. Goncharevich I. F., Vibrations – A Non Standard Approach. (Academy of Science of USSR Publishing House Nauka, 1986, Moscow, 204 pages, in Russian).
- [4]. Chernousko F.L., About the motion of a body containing internal moving mass. // (Conference Paper published by the Russian Academy of Science, Vol. 405, №1, p. 1-5, 2005, in Russian).
- [5]. Lupehina, I.V., A study of a Mobile Vibration System, moving with a Breakaway from the surface. Journal of Computer and System Sciences International, Vol. 50, No. 2, 2011, pp.336-347
- [6]. Lupehina, I.V., Modelling of Hopping Robot with Active Vibro-isolation for on Board equipment. Proceedings of (CLAWAR) 12-th International Conference on Climbing and Walking Robots and their Supporting Technologies. Istanbul, 2009, Turkey, pp. 869-876.
- [7]. Jatsun C.F., Volkova L. Ju., Modelling of the dynamic regimes of a vibration robot moving on a surface with fluid friction. Journal of Superior Technics & Communications, Vol. 3, 2012, pp. 23-29 (in Russian).
- [8]. Provatidis Ch. G., Mechanics of Dean Drive on Frictional Grounds. Journal of Mechanical Design and Vibrations, Vol. 1, No. 1, 2013, pp. 10-19, Science and Publication Publishing. Available on <http://pubs.sciepub.com/jmdv/1/1/3>, DOI:10.12691/jmdv/1/1/3.
- [9]. Provatidis Ch. G., Design of A Propulsion Cycle for Endless Sliding on Frictional Ground Using Rotating Masses, Universal Journal of Mechanical Engineering Vol. 2 (2): 35-43, 2014. Available on [http://www.hrpub.org/journals/article\\_info.php?aid=1245](http://www.hrpub.org/journals/article_info.php?aid=1245), DOI: 10.13189/ujme.2014.020201.
- [10]. Jatsun C.F., Mishchenko V. Ja., Russian Patent No. 88639, MPK B62D 57/00. Vibration propeller.
- [11]. Jatsun S. F., Bolotnik N., Zimmerman K., Zeidis I., Modeling of Motion of Vibrating Robots, 12-th IFToMM World Congress, Besançon (France), June 18-21, 2007.